RI | 9236

REPORT OF INVESTIGATIONS/1989

Structural Stability and Oxidation Resistance of Substitute Alloys With Various Cr and Mn Levels

By Je M. Oh and Max L. Glenn

BUREAU OF MINES

UNITED STATES DEPARTMENT OF THE INTERIOR

Report of Investigations 9236

Structural Stability and Oxidation Resistance of Substitute Alloys With Various Cr and Mn Levels

By Je M. Oh and Max L. Glenn

UNITED STATES DEPARTMENT OF THE INTERIOR
Manuel J. Lujan, Jr., Secretary

BUREAU OF MINES
T S Ary, Director

Library of Congress Cataloging in Publication Data:

Oh, Je M. (Je Myung)
Structural stability and oxidation resistance of substitute alloys with various Cr and Mn levels.

(Report of investigations; 9236)

Bibliography: p. 11.

Supt. of Docs. no.: I 28.23:9236.

1. Chromium-iron alloys. 2. Iron-manganese alloys. 3. Steel, Stainless. 4. Stability. 5. Oxidation. I. Glenn, M. L. (Max L.). II. Title. III. Series: Report of investigations (United States. Bureau of Mines); 9236.

TN23.U43 [TN693.I7] 622 s [672] 88-600353

CONTENTS

ILLUSTRATIONS

TABLES

UNIT OF MEASURE ABBREVIATIONS USED IN THIS REPORT

°C	degree Celsius	mg/cm^2	milligram per square centimeter
cm	centimeter	mm	millimeter
g	gram	μm	micrometer
h	hour	pct	percent
kV	kilovolt	wt pct	weight percent

STRUCTURAL STABILITY AND OXIDATION RESISTANCE OF SUBSTITUTE ALLOYS WITH VARIOUS Cr AND Mn LEVELS

By Je M. Oh[1] and Max L. Glenn[2]

ABSTRACT

The U.S. Bureau of Mines is conducting research on the oxidation resistance and structural stability of Fe-(0-8)Cr-(0-16)Ni-(0-16)Mn-3.5Si-1Al alloys as potential substitutes for high-Cr stainless steels. Oxidation tests were conducted in air over the temperature range of 600° to 900° C for up to 1,000 h. Microstructures were analyzed at room temperature after hot rolling. The oxidation properties and the structural stability were found to be greatly affected by the Cr and Mn levels. Although substitution of Mn for Ni increased the oxidation rate, the Mn helped to stabilize the austenitic microstructure. Decreasing the Cr content or increasing the Mn content produced higher oxidation rates and earlier oxide spalling. In this study, reaction kinetics, oxide morphologies, and microstructure of the alloys were investigated using scanning electron microscopy, energy dispersive X-ray analysis, X-ray diffraction, and electron microprobe analysis.

[1]Supervisory metallurgist.
[2]Metallurgist.
Albany Research Center, U.S. Bureau of Mines, Albany, OR.

INTRODUCTION

Because Cr is considered a vulnerable strategic metal, the Bureau of Mines is investigating reduced-Cr substitute alloys. Commercial AISI Type 304 stainless steel (SS) and similar stainless steels account for a major percentage of the Nation's Cr consumption (*1*).[3] Therefore, this research is concentrated on developing a low-Cr (8 pct) substitute for Type 304 SS (*2-7*). Suitable substitutes for Type 304 SS must possess good mechanical properties and good oxidation resistance. To lower the Cr content while maintaining the oxidation resistance similar to that of stainless steels, elements such as Al and/or Si must be added. Because the alloys with reduced-Cr contents develop a martensitic microstructure, the desired austenitic microstructure must be stabilized in these substitute alloys by additions of at least 15 pct Ni.

High concentrations of Cr (>15 pct) are used in commercial stainless steels to provide a protective and self-healing oxide surface. When the Cr content is lower than 13 pct, some of the Fe is oxidized along with the Cr, forming a less protective layer (*8*). Reduction of the Cr concentration below 10 pct results in the formation of an inner layer of $(Fe, Cr)_3O_4$ and an outer layer of $(Fe, Cr)_2O_3$ (*9*).

Aluminum-containing M-Cr-Al alloys (M = Fe, Co, or Ni) form a continuous protective Al_2O_3 layer or a duplex layer of Al and other metal oxides depending upon the temperature, oxidation environment, and the concentrations of Al and Cr (*10-13*). Chromium in these alloys acts either to (1) getter the oxygen, (2) stabilize the α-Al_2O_3, or (3) limit internal oxidation (*14-16*). Generally, such M-Cr-Al alloys are designed for higher temperatures (i.e., >1,000° C), where the Cr oxide starts to form a volatile CrO_3.

The beneficial effect of Si on high-temperature oxidation has been reported by many investigators (*17-25*). Silicon forms a thin, continuous or semicontinuous SiO_2 layer at the metal-scale interface. The SiO_2 reduces the inward and outward diffusion of oxygen and metal ions so that the oxidation resistance is greatly improved.

Previous Bureau research shows that an Fe-16Ni-8Cr-3.5Si-1Al alloy has excellent oxidation resistance at temperatures as high as 900° C (*4-5, 7*). A mixed austenitic-martensitic microstructure was observed in this alloy at room temperature. Increasing the Al content of this alloy resulted in poor fabricability and deeper penetration of internal oxidation. When Mo was added to a similar alloy, silicides formed that increased the oxidation resistance (*26*).

In this report, the effects of the variation of Cr, substitution of Mn for Ni, and addition of Mo were evaluated for comparison with an Fe-16Ni-8Cr-3.5Si-1Al base alloy. Various Cr levels, from 8 to 0 pct, were examined to determine the minimum Cr content required for oxidation resistance and the effect of reduced Cr levels on microstructure. Manganese was substituted for Ni to determine its effect on stabilization of the austenite and on oxidation resistance. Molybdenum was added because of its known ability to stabilize austenite and to enhance oxidation resistance.

EXPERIMENTAL PROCEDURE

Alloys were produced from electrolytic grades of Fe, Cr, Ni, Mo, FeSi, and high-purity Al. These charge materials were vacuum arc melted into 100-g buttons in an argon atmosphere. The buttons were homogenized in a vacuum for 20 h at 1,200° C and then hot rolled to 2-mm sheets at 1,100° C with 20-pct reduction per pass. The oxidation specimens were cut from the sheets, polished to 600 grit, ultrasonically cleaned, and then degreased with acetone and alcohol. The 1.5- by 2-cm oxidation specimens were placed on a quartz rack and oxidized in static air. Experimental times and temperatures ranged up to 1,000 h at 600° to 900° C. The specimens were periodically taken out of the furnace and weighed to determine the weight gain during oxidation. After oxidation, the specimens were analyzed with an optical microscope, X-ray diffractometer, scanning electron microscope (SEM), electron microprobe, and energy dispersive X-ray analyzer (EDXA). Nominal alloy compositions are presented in table 1. The analyzed alloy compositions showed that all alloying elements were very close to the nominal compositions (less than ±3 pct), except for Si. Silicon was 6 to 8 pct less than the nominal compositions.

[3]Italic numbers in parentheses refer to items in the list of references at the end of this report.

Table 1.—Nominal alloy composition,[1] percent

Alloy	Cr	Ni	Mn
A	0	16	0
B	2	16	0
C	4	16	0
D	6	16	0
E	8	16	0
F	8	12	4
G	8	8	8
H	8	4	12
I	8	0	16
J[2]	8	8	8

[1]Fe-3.5Si-1Al base.
[2]Contains 2 pct Mo.

RESULTS

The experimental results are presented in the following three sections: (1) microstructure of alloys, (2) oxidation reaction kinetics, and (3) oxide scale morphology and composition.

MICROSTRUCTURE OF ALLOYS

The microstructures of an Fe-8Cr-16Ni-3.5Si-1Al base alloy with various modifications are shown in figures 1, 2, and 3. Figure 1 shows the microstructures that resulted from varying the Cr content. The alloys with Cr contents of up to 8 pct Cr contained lath martensite. An additional alloy containing 12 pct Cr also was produced, which had an austenitic microstructure. The effects of a one-for-one replacement of Ni with Mn in the Fe-8Cr-16Ni-3.5Si-1Al base alloy are shown in figure 2. The alloy containing 12Ni-4Mn was the alloy that had the largest austenite content. The 16-Ni alloy contained lath martensite, while the Mn-rich alloys contained sheet martensite. The microstructure of an Fe-8Cr-8Ni-8Mn-3.5Si-1Al-2Mo alloy is shown in figure 3. The alloy with Mo additions was austenitic; however, the alloy without the Mo addition was martensitic (not included in figure).

OXIDATION REACTION KINETICS

Figure 4*A* shows the reaction kinetics of alloys oxidized up to 500 h at 600° C. Each data point represents a time when the specimen was cooled to room temperature, weighed, then replaced in the furnace. Alloys A, B, C, D, and E had negligible weight changes; therefore, they are not included here. Oxidation of alloys F, G, H, I, and J obeyed the cubic rate law. The oxidation rate increased when the Mn content increased. Additions of Mo helped to reduce the oxidation rate. Alloy J, which contained 2 wt pct Mo, showed better oxidation resistance than alloy G, which had no Mo. Thermal cycling, caused when the specimens were cooled for weighing, did not promote any spalling.

Figure 4*B* shows the reaction kinetics of alloys oxidized for 1,000 h at 700° C; Type 304 SS was included for comparison. Alloy A formed oxide blisters during 100 h of oxidation. Alloys B, C, D, and E had extremely small weight gains, much lower than that of Type 304 SS. However, the oxidation rate increased when the Mn content increased. Manganese-containing alloys (i.e., alloys F, G, H, I, and J) showed higher oxidation rates than did Type 304 SS. Alloy I, which contained 16 wt pct Mn, showed the highest weight gains.

Figure 4*C* shows the weight changes of alloys oxidized at 800° C. Alloy A formed oxide blisters during 13 h of oxidation. Alloys B and C, D and E, and F and J had identical reaction rates. Alloys H and I showed spalling after 1,000 and 100 h of oxidation, respectively.

Figure 4*D* shows the weight changes of the alloys at 900° C. Alloys G and J showed the same oxidation rate until alloy G (not shown in figure 4*D*) began to spall after 30 h. Alloy J spalled after 300 h of oxidation. The data indicate that the additions of Mo did not improve oxidation resistance but seemed to help the oxide adherence. At 900° C, oxidation of the alloys obeyed a parabolic rate law. More detailed explanation will be given in the "Discussion" section.

Throughout the oxidation reaction, some general trends were observed:

1. Oxidation rate increased with higher Mn contents.

2. There was earlier spalling with higher Mn contents or reduced Cr contents.

3. Different rate laws were observed with different alloy compositions and temperatures.

4. Molybdenum additions improved oxidation protection and scale adherence.

MORPHOLOGY AND COMPOSITION OF OXIDE

The morphology and composition of the oxide scale were examined with optical microscopy, SEM, EDXA, X-ray diffractometer, and the electron microprobe.

At 700° C, alloy A formed oxide nodules, particularly along the edge of the specimen. These nodules contained more than 90 pct Fe as determined by EDXA. Alloys B, C, D, and E, with 2, 4, 6, and 8 pct Cr, did not form any visible nodules and still showed some degree of metallic shine after 1,000 h of oxidation. Figure 5 shows the SEM photomicrographs of the oxides that formed on alloys E, F, G, and J after 1,000 h of oxidation at 700° C. When Mn was substituted for Ni in these alloys, oxide nodules formation increased. Nodule size and thickness of the oxide layer increased when the Mn content increased. Alloy E did not form any nodules nor did it have a thick enough oxide layer to cover the polishing grooves. Alloy F formed oxide nodules that did not completely cover the surface. Energy dispersive X-ray analyses of nodules and surface areas are presented in table 2. The nodules contained mainly Mn, while the areas between the nodules had compositions similar to those of the base alloy. Apparently the Mo addition affects the oxide morphology, because alloy J formed smaller oxide nodules than did alloy G. In these alloys, the oxide nodules formed and grew along the polishing grooves.

Figure 6 shows an SEM photomicrograph of alloy J after 72 h of oxidation at 800° C. The globular oxide nodules protruded through the base oxide. These nodules contained more than 95 pct Mn as determined by EDXA

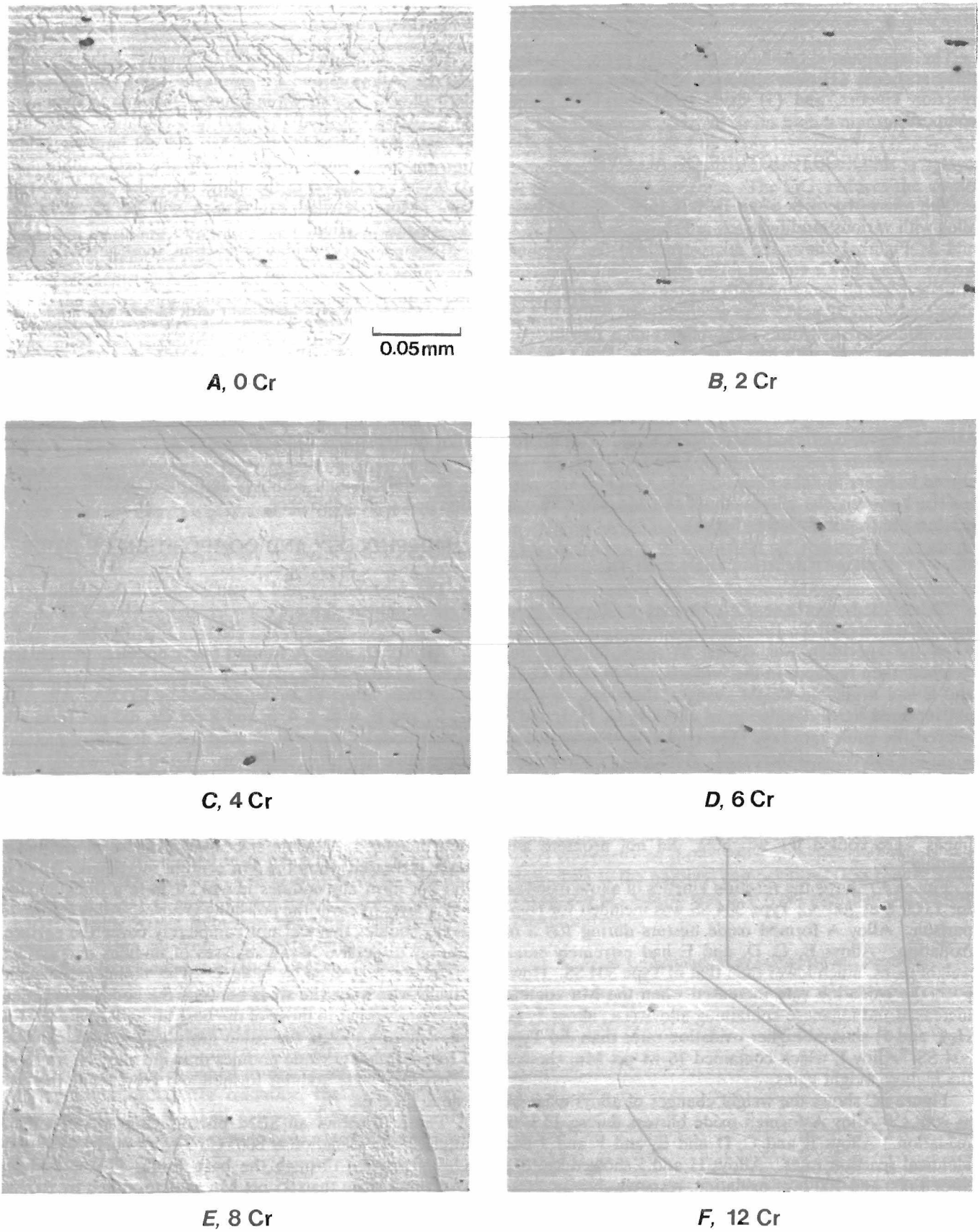

Figure 1.—Effects of Cr on microstructure of Fe-Cr-16Ni-3.5Si-1Al alloys.

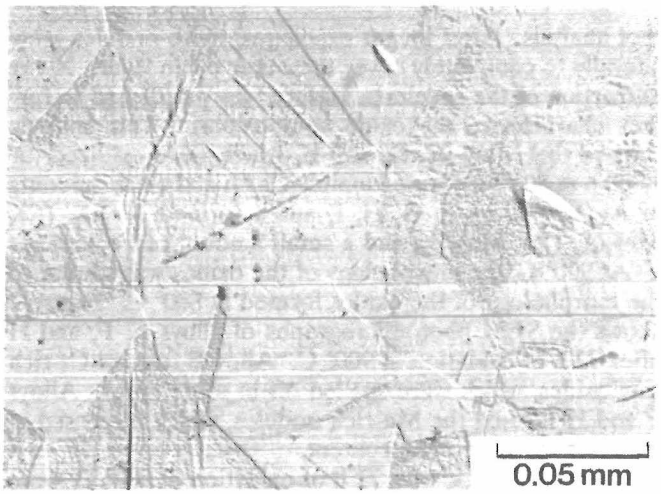

A, 16 Ni

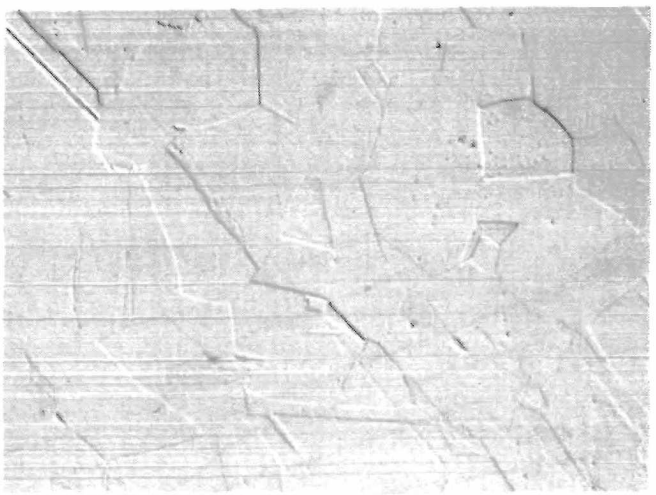

B, 12 Ni - 4 Mn

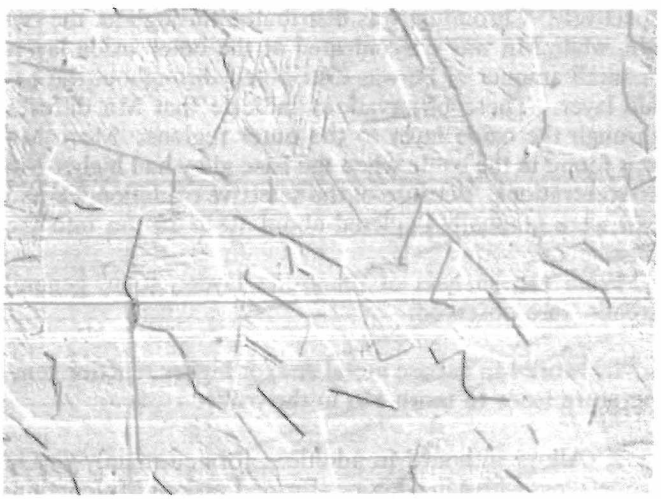

C, 8 Ni - 8 Mn

D, 4 Ni - 12 Mn

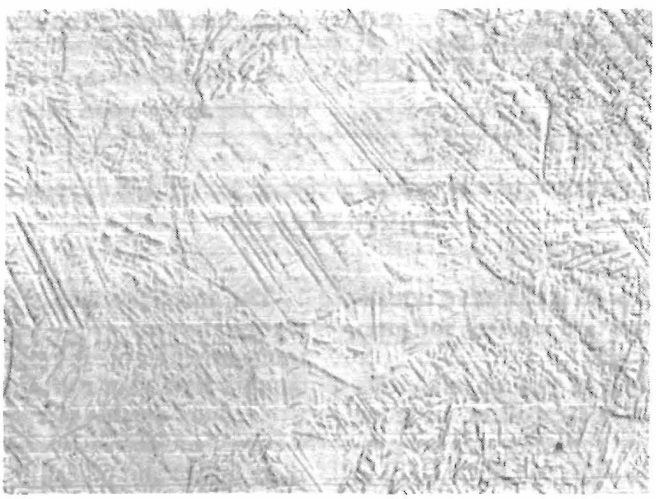

E, 16 Mn

Figure 2.—Effects of substituting Mn for Ni in Fe-8Cr-16Ni-3.5Si-1Al alloy.

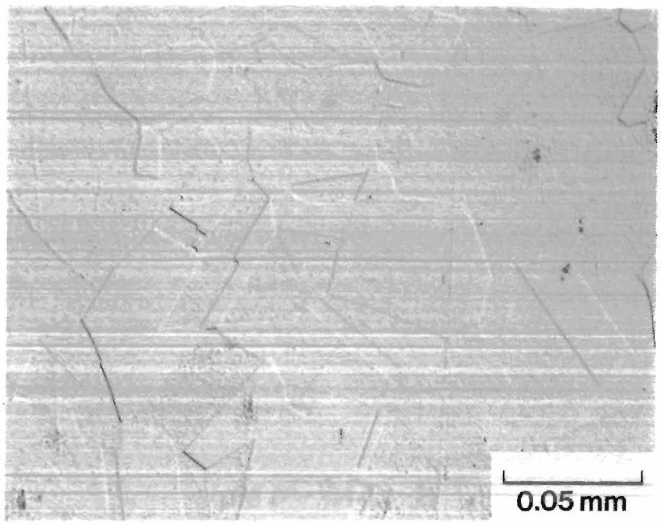

Figure 3.—Effect of Mo additions on Fe-8Cr-8Ni-8Mn-3.5Si-1Al-2Mo alloy.

Table 2.—Energy dispersive X-ray analyses of nodules and oxidized surfaces

Alloy	Fe	Cr	Ni	Mn	Si	Al
			700° C, 1,000 h			
F[1]	71.26	7.31	8.97	8.10	0.62	3.74
F[2]	4.26	11.86	.71	80.30	1.07	1.81
G[3]	5.53	16.40	1.03	73.11	.87	2.24
H[3]	2.74	11.27	.31	84.63	.43	.61
I[3]	.5	4.41	.35	93.04	.55	1.15
J[3]	11.03	21.98	2.31	59.99	1.07	3.62
			800° C, 72 h			
G	3.97	16.17	ND	78.54	ND	1.31
J	23.74	27.19	1.98	43.73	0.7	2.14
			900° C, 72 h			
E	52.38	21.49	12.58	ND	3.00	10.54
F	5.45	30.12	.8	58.09	.92	4.61
G	3.41	8.78	ND	84.94	1.15	1.73
H	.71	7.62	ND	90.43	.33	.91
J	3.12	15.65	.61	77.21	1.37	2.05

ND Not detected. [2]Oxide nodule.
[1]Beside nodule. [3]Oxide surface.

spot analysis. After longer exposures, these nodules grew laterally to completely cover the outer oxide layer. X-ray diffraction of the specimen surface was performed to further characterize the oxide composition. This analysis showed that alloys C, D, and E, which were oxidized for 1,000 h at 800° C, formed mainly Cr_2O_3 and trace amounts of Al_2O_3. Alloys F, G, H, I, and J formed Mn_2O_3, $(Cr, Mn)_2O_3$, $(Fe, Mn)_2O_3$, and a small amount of Fe_2MnO_4.

At 900° C, the morphology of the oxides was similar to the morphology of the oxides formed at 800° C. Figure 7 shows the SEM photomicrographs of alloys E, F, and H after 72 h of oxidation at 900° C. Alloy E formed Cr-rich thin oxides, which were spalled off in some areas. Alloys F and H formed the Mn-rich nodules, which increased in size with increased Mn content.

Alloys F and G, with 72 h of oxidation at 900° C, were mounted in epoxy, cross-sectioned, then examined by electron microprobe to obtain elemental profiles. Figure 8 shows the Cr, Fe, and Mn profiles of alloys F and G, respectively. Chromium was distributed throughout the oxide, while Mn was concentrated at the outer oxide layer. A small amount of Fe was distributed throughout the oxide layer. These observations indicate that Mn diffuses through the oxide layer to the outer regions. More Mn was found in the oxide when the base alloy had higher Mn concentrations. Because of the selective oxidation, Cr and Mn were gradually depleted about 10 to 20 μm into the base metal.

From the analysis of the oxide layers, some general trends were observed:

1. More Mn in base metal and/or higher reaction temperature leads to more Mn in the oxide.

2. Alloys without Mn additions formed mainly Cr_2O_3, while alloys with Mn additions formed various Mn-containing oxides.

3. Alloy J (Mo added) had more Cr and less Mn in the oxide than alloy G (no Mo added).

4. The size of the nodules and the thickness of the oxides depended upon Mn contents in the alloys.

DISCUSSION

The effects of Cr and Mn in low-Cr steels were investigated based on microstructure, reaction kinetics, and morphology of the oxide and base metal.

Previous Bureau research showed that an alloy that contained Fe-8Cr-16Ni-3.5Si-1Al had excellent oxidation resistance up to 900° C. However, this alloy was not austenitic at room temperature. The variation of Cr and Mn contents in the alloys affects the microstructure and oxidation properties of the alloys.

The microstructure of the alloys is dependent upon the martensite-start (Ms) temperature, which controls the transformation of austenite to martensite. Previous investigators have shown that all alloying constituents, except Co, reduce the Ms temperature (*27*). Therefore, unlike the austenite-ferrite equilibrium where some elements promote ferrite and others promote austenite, the addition of alloying elements, except Co, inhibits martensitic transformation and promotes the austenitic stability. The

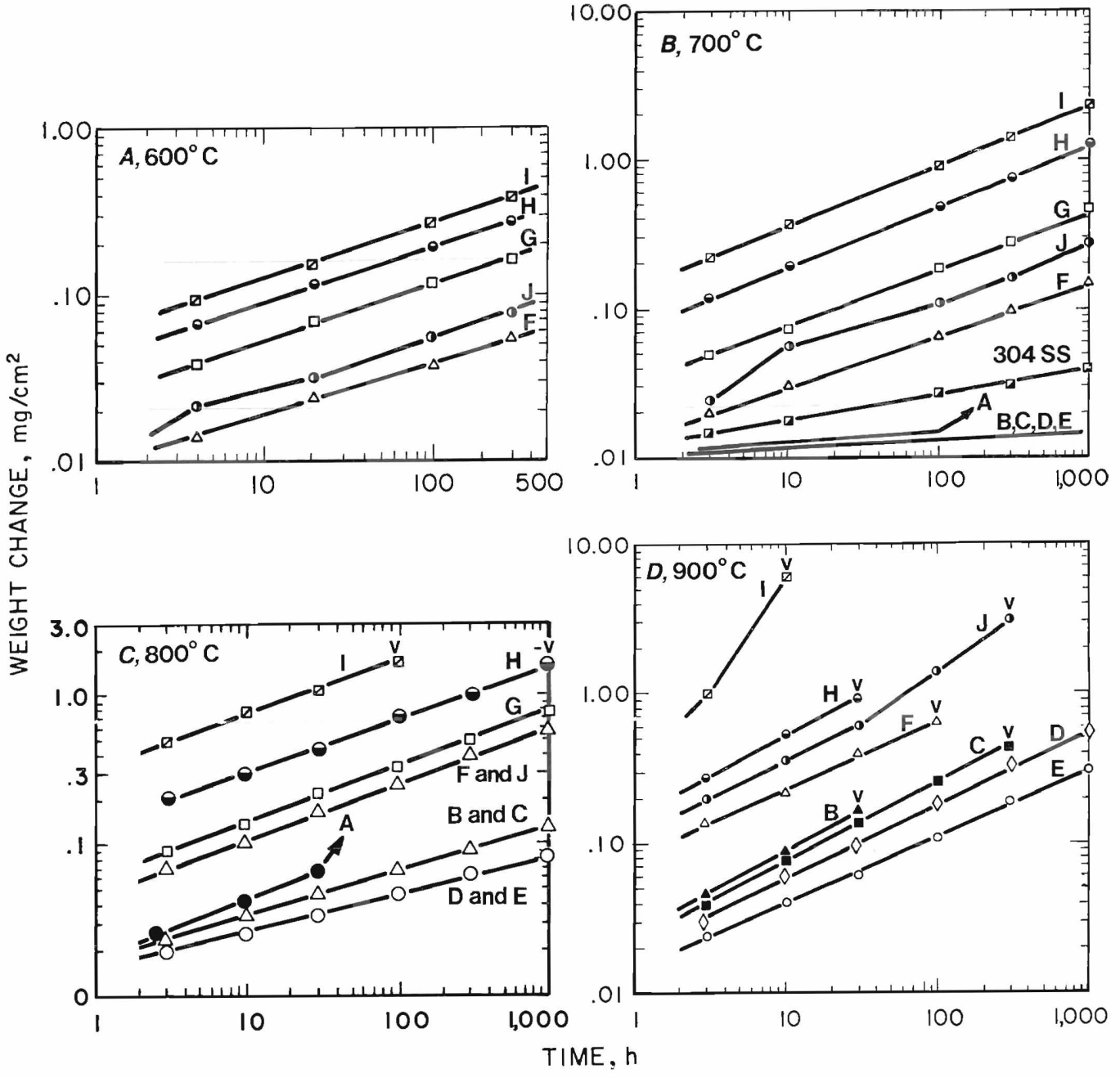

Figure 4.—Reaction kinetics of alloys plotted on log-log scale at various temperatures. (V indicates spalling.)

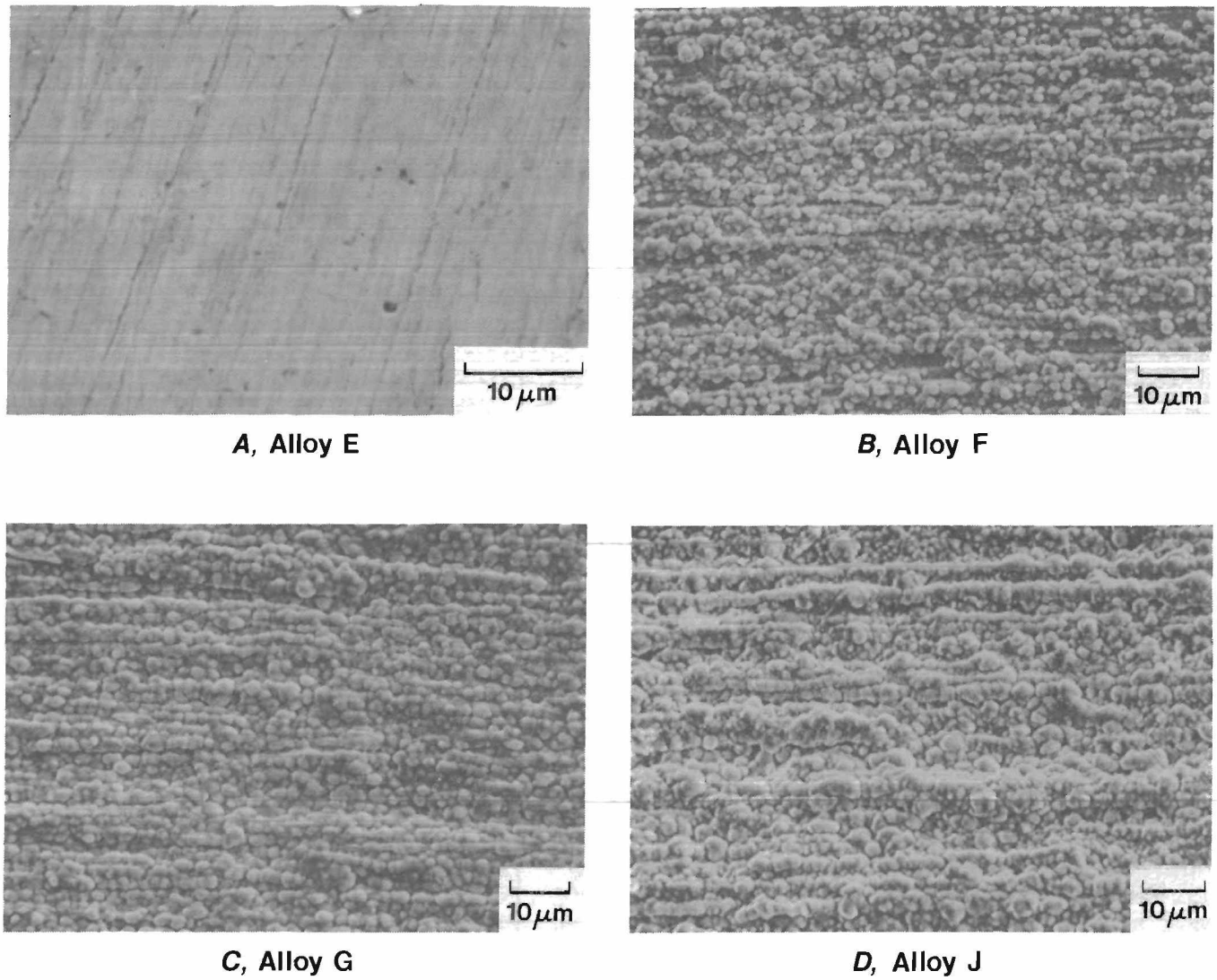

A, Alloy E

B, Alloy F

C, Alloy G

D, Alloy J

Figure 5.—Surface morphology of alloys after 1,000 h of oxidation at 700° C. (20 kV.)

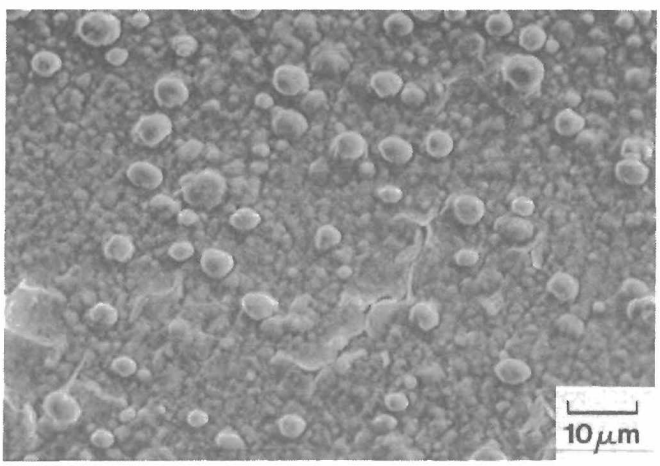

Figure 6.—Surface morphology of alloy J after 72 h of oxidation at 800° C. (20 kV.)

results shown here are in agreement with these martensitic transformation generalities. Because the 12-pct-Cr alloy was the only alloy in figure 1 with an austenitic microstructure, Cr seems to enhance the stability of austenite. In figure 3, Mo is shown to stabilize the austenitic microstructure. Furthermore, figure 2 shows that neither 16 pct Ni nor 16 pct Mn sufficiently stabilizes austenite. The substitution of Mn for Ni stabilizes the austenite for low additions (i.e., 12Ni-4Mn) but promotes the transformation from lath martensite to sheet martensite at high Mn levels. Such response may indicate separate Ms relationships for the formation of lath versus sheet martensite.

The reaction kinetics and the oxide morphologies were consistent. The alloys that showed low oxidation rates formed thin oxide layers. Alloys without Mn additions had small weight gains, while alloys with Mn additions had large weight gains. The minimum Cr contents necessary to provide oxidation resistance depended upon the

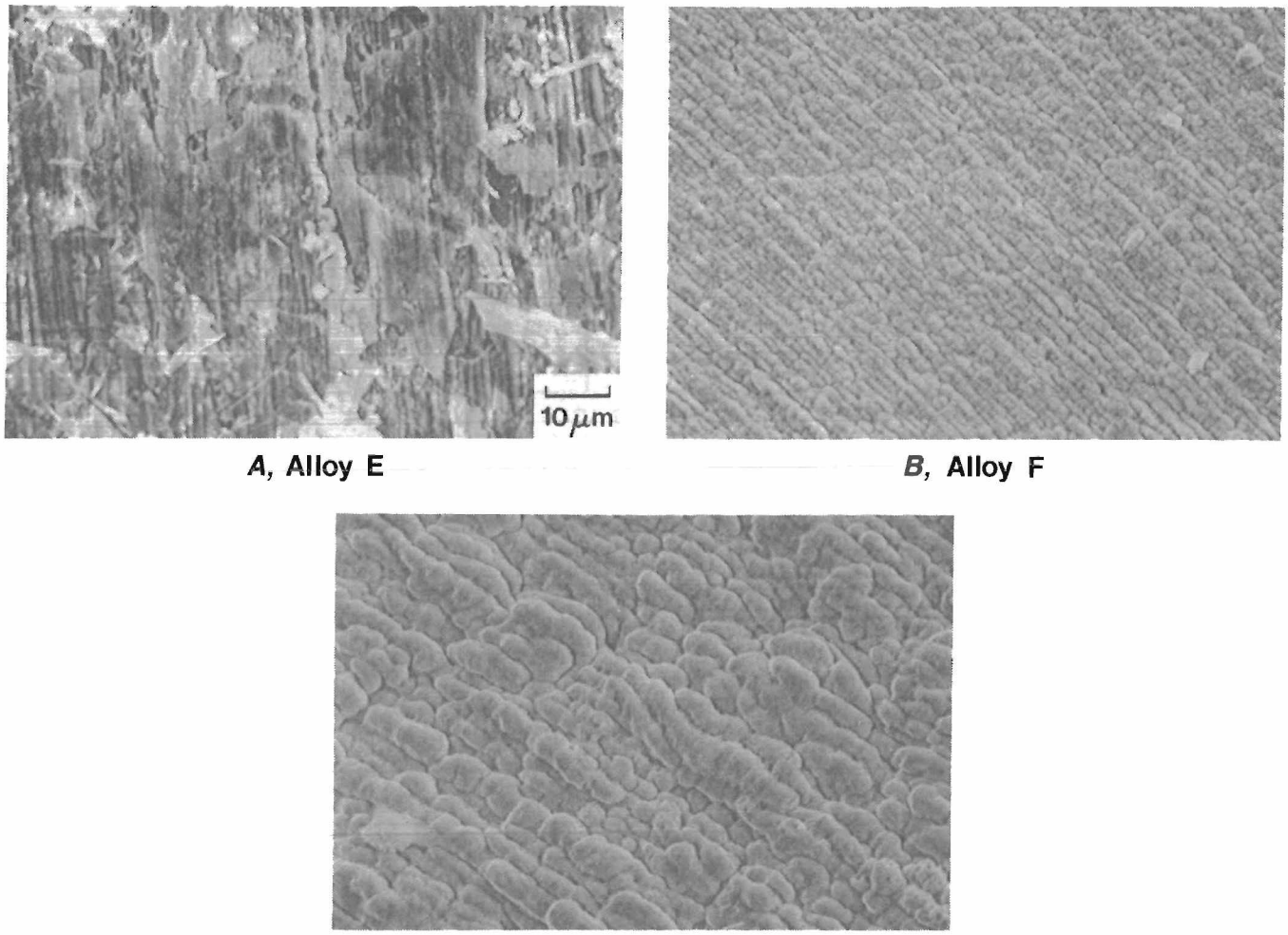

Figure 7.—Surface morphology of alloys after 72 h of oxidation at 900° C. (20 kV.)

oxidation temperature and time. The experimental data indicate that approximately 2 to 6 pct Cr provided oxidation protection for the alloys that did not contain Mn at 700° to 900° C in laboratory tests up to 1,000 h. However, these Cr contents may not be enough for longer exposures or severe thermal cyclings during oxidation in practical use. Therefore, the addition of more Cr or lowering the operating temperature should be considered for practical use. Since Cr is the main element to form a protective external oxide layer, it is important to maintain amounts of Cr sufficient to reform a protective layer when the oxide layer is cracked.

Substitution of Mn for Ni causes a significant change in oxidation rate and oxide morphology. Manganese is used as an impurity getter during steelmaking; it stabilizes the austenitic microstructure; and it is cheaper than Ni. Although partial Mn substitution for Ni helped to increase austenite content in the alloys, Mn substitution for Ni was detrimental to oxidation protection. The rapid diffusion of Mn ions through the oxide creates vacancy gradients to increase the oxidation rates. Although alloy F showed a somewhat higher oxidation rate than did Type 304 SS at 700° C, the oxidation rate was acceptable. Alloys that contained 4 wt pct Mn or more showed oxidation rates higher than Type 304 SS and had less austenite content. Therefore, alloys G, H, and I may not be suitable for practical use.

Molybdenum has been known to lower the Ms temperature and hence stabilize the austenitic microstructure. The addition of Mo in this investigation was very effective in improving the oxidation resistance and increasing the austenite content of the alloy. Also, Mo has been known to decrease the diffusion of metal ions through grain boundaries, as well as the lattice, because of the size effect (*28*). Consequently, a slow oxidation rate was observed in previous investigations (*7, 26*). In this study, alloy J, which contained 2 wt pct Mo, showed higher austenite content and better oxidation resistance than alloy G, which contained no Mo.

The oxidation rate laws depend upon the alloy compositions and reaction temperatures. Alloys A, B, C, D, and E had extremely small weight gains at lower temperatures

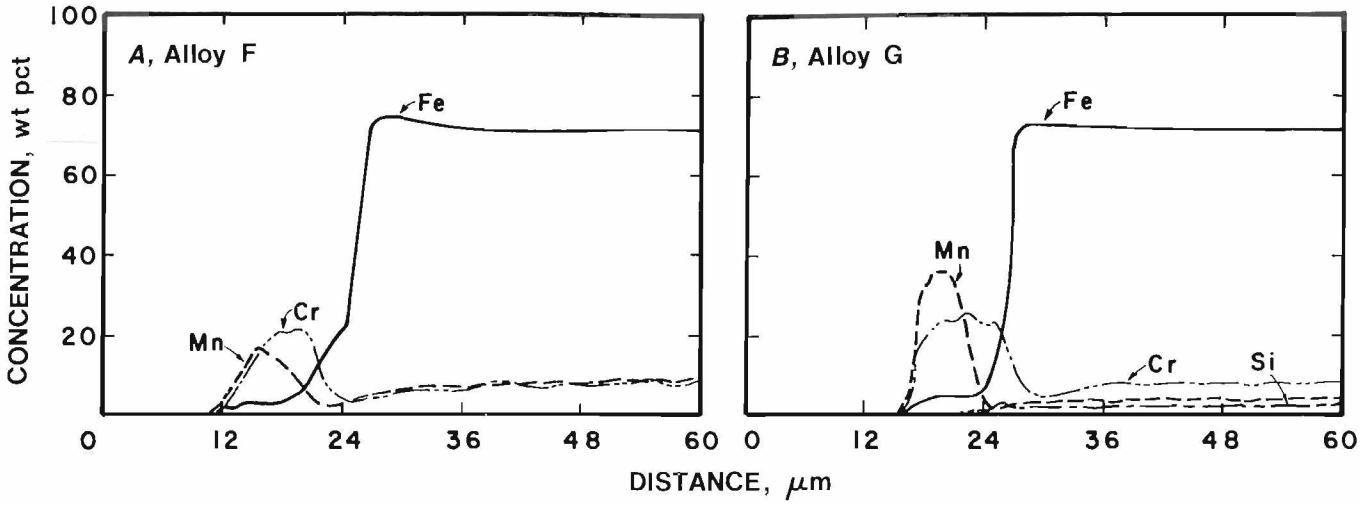

Figure 8.—Concentration profiles near metal-scale interface after 72 h of oxidation at 900° C by electron microprobe.

(600° and 700° C); therefore, it was not possible to determine which rate law applied. These alloys clearly obey parabolic rate laws at 900° C. This temperature is high enough to form considerable Cr_2O_3. The Cr content seems to have an effect on the oxide adherence. The lower Cr-containing alloys had earlier spalling.

Alloys F, G, H, I, and J have slopes ranging from 0.34 to 0.4, which means that these alloys obey or are close to cubic rate law kinetics. The cubic rate law is observed in high-temperature oxidation of alloys when the composition of the oxide scale changes with time. The data show that these alloys form various oxides and the oxide compositions do change with time. Indeed, more Mn-containing oxides were observed with longer oxidation.

CONCLUSIONS

The microstructures and oxidation properties of the alloys were greatly affected by the concentrations of alloying elements. Several features were observed with various Cr and Mn levels in the alloys tested:

1. When Cr concentration increases, the alloys show better oxidation protection, less weight gain, and better oxide adherence.

2. When Mn is substituted for Ni, higher oxidation rates and earlier oxide spalling are observed with higher Mn content. However, addition of 4 wt pct Mn helps to stabilize the austenitic microstructure.

3. Addition of Mo into the alloy improves oxidation protection and stabilizes the austenitic microstructure.

REFERENCES

1. National Materials Advisory Board. Contingency Plans for Chromium. Natl. Acad. Sci., Washington, DC, NMAB-335, 1978, 311 pp.

2. Dunning, J. S., H. W. Leavenworth, and M. L. Glenn. Substitutes for Chromium in Stainless Steel. Met. Prog., v. 126, No. 5, 1984, 19 pp.

3. Glenn, M. L., D. E. Larson, S. J. Bullard, and S. C. Rhoads. Partial Replacement of Chromium in Stainless Steel. J. Mater. Energy Syst., v. 7, June 1985, pp. 75-81.

4. Oh, J. M. Effect of Alloying Elements on Oxidation of Low-Chromium Alloys. BuMines RI 9047, 1986, 12 pp.

5. Rawers, J. C., and D. E. Larson. Oxidation of Fe-8Cr-14Ni-Al-Si-Mn from 700 to 1,000° C. Oxid. Met., v. 27, 1987, pp. 103-120.

6. Dunning, J. S., J. M. Oh, and J. C. Rawers. An Assessment of Possible Substitutes for Chromium in Stainless Steels. Paper in Proceedings, Alternate Alloying for Environmental Resistance. Met. Soc., 1987, pp. 3-11.

7. Oh, J. M. Development of Low-Chromium Substitute Alloys for High-Temperature Applications. J. Electrochem. Soc., v. 135, 1988, pp. 749-755.

8. Kuroda, J., P. A. Labun, G. Welsch, and T. E. Mitchell. Oxide Formation Characteristics in the Early Stages of Oxidation of Fe and Fe-Cr Alloys. Oxid. Met., v. 19, 1983, pp. 117-128.

9. Francis, J. M. Influence of Minor Alloying Elements on Structure of Surface Oxides Forming During the High Temperature Oxidation of an Austenitic Steel. J. Iron and Steel Inst., London, v. 204, 1966, p. 140.

10. Wood, G. C. High Temperature Oxidation of Alloys. Oxid. Met., v. 2, 1970, pp. 11-57.

11. Stott, F. H., G. C. Wood, and M. G. Hobby. A Comparison of the Oxidation Behavior of Fe-Cr-Al, Ni-Cr-Al, and Co-Cr-Al Alloys. Oxid. Met., v. 3, 1971, pp. 103-113.

12. Wood, G. C. and F. H. Stott. The Influence on the Oxidation of Co-Cr Alloys at 1,000 and 1,200° C of Aluminum Additions. Oxid. Met., v. 3, 1971, pp. 365-398.

13. Stott, F. H., and G. C. Wood. The Mechanism of Oxidation of Ni-Cr-Al Alloys. Corros. Sci., v. 11, 1971, pp. 799-812.

14. Miner, R. G., and V. Nagarajan. The Morphology of Oxidation of Alumina-Forming Iron-Base Chromium and Silicon. Oxid. Met., v. 16, 1981, pp. 295-326.

15. Wagner, M. C. Passivity and Inhibition During the Oxidation of Metals at Elevated Temperatures. Corros. Sci., v. 5, 1965, pp. 751-764.

16. Hagel, W. C. The Oxidation of Iron, Nickel, and Cobalt-Base Alloys Containing Aluminum. Corrosion (Houston), v. 21, 1965, pp. 316-326.

17. Evans, J. W., and S. K. Chatterji. Influence of Silicon on the High-Temperature Oxidation of Copper and Iron. J. Electrochem. Soc., v. 106, 1959, pp. 860-866.

18. Logani, R., and W. W. Smeltzer. Kinetics of Wustite-Fayalite Scale Formation on Iron-Silicon Alloys. Oxid. Met., v. 1, 1969, pp. 3-21.

19. Svendung, I., and N. G. Vannerberg. The Influence of Silicon on the Oxidation Properties of Iron. Corros. Sci., v. 14, 1974, pp. 391-400.

20. Douglass, D. L., and J. S. Armijo. The Effect of Silicon and Manganese on the Oxidation Mechanism of Ni-20Cr. Oxid. Met., v. 2, 1970, pp. 207-231.

21. Jones, D. E., and J. Stringer. The Effect of Small Amount of Silicon on the Oxidation of High-Purity Co-25Cr at Elevated Temperatures. Oxid. Met., v. 9, 1975, pp. 409-413.

22. Kumar, A., and D. L. Douglass. Modification of the Oxidation Behavior of High-Purity Austenitic Fe-14Cr-14Ni by the Addition of Silicon. Oxid. Met., v. 10, 1976, pp. 1-22.

23. Bogg, W. E. The High-Temperature Oxidation Resistance of Iron-Silicon-Aluminum Alloys. Oxid. Met., v. 10, 1976, pp. 277-290.

24. Yurek, G. J., D. Eisen, and A. Garratt-Reed. Oxidation Behavior of a Fine Grained Rapidly Solidified 18-8 Stainless Steel. Metall. Trans. A, v. 13A, 1982, pp. 473-485.

25. Evans, H. E., D. A. Hilton, R. A. Holm, and S. J. Webster. Influence of Silicon Additions on the Oxidation Resistance of a Stainless Steel. Oxid. Met., v. 19, 1983, pp. 1-18.

26. Rawers, J. C. Inherent Oxidation Protection of Fe-5Cr-15Ni-2Si-4.5Mo. Oxid. Met., v. 28, 1987, pp. 183-194.

27. Kung, C. Y., and J. J. Rayment. An Examination of the Validity of Existing Empirical Formulas for the Calculation of Ms Temperature. Metall. Trans. A, v. 13A, 1982, pp. 328-331.

28. Meier, G. H., and F. S. Pettit. High Temperature Oxidation of Rapidly Solidified Ni-Mo-Al-W Alloys. Paper in Proceedings of Third Conference on Rapid Solidification Processing (Dec. 6-8, 1982), ed. by R. Mehrabian. NBS, 1983, pp. 348-359.

* U.S. GOVERNMENT PRINTING OFFICE: 611-012/00,059

INT.-BU.OF MINES,PGH.,PA. 28887